Critical Currents in Superconducting Tin and Indium*

Peter Scharnhorst

U.S. Naval Ordnance Laboratory, Silver Spring, Maryland 20910

(Received 9 July 1969; revised manuscript received 26 August 1969)

The critical current densities in planar superconducting films of tin and indium were determined as a function of temperature by using a new method. An alternating current in a flat ribbon-shaped drive loop was imaged in the superconducting film. Both tin and indium films were deposited at 80 °K and were annealed to temperatures between 80 and 180 °K. The temperature dependence of $J_c(t)$ was found to be $(1 - t^2)^\alpha (1 + t^2)^{1/2}$, where $\alpha = 1.23$ for tin and $\alpha = 1.16$ for indium.

I. INTRODUCTION

Several attempts have been made in recent years to measure the critical current density of thin superconducting films.[1-9] The results of different experiments generally disagree both in magnitude and with respect to the temperature dependence of this current. Theoretical studies indicate that the temperature dependence near T_c should be $(1 - t)^{3/2}$.[10-13] Amplitudes are predicted to be typically of the order of 10^6–10^7 A/cm² in vacuum-evaporated thin films near absolute zero. Depending on the particular experimental arrangement as well as on sample preparation procedure, experimenters have measured temperature dependences ranging from $(1 - t)^{0.6}$ to $(1 - t)^{2.3}$ near T_c.[3,7] Magnitudes have generally been low compared to theoretical estimates, except for those of Glover and Coffey[6] and Hunt.[9] These authors report excellent agreement with theory near T_c but they disagree on the form of the temperature dependence at lower temperatures.

The difficulties with this type of experiment can be traced to essentially three different causes: inhomogeneities in the sample, heating via contact resistance if the current is injected rather than induced, and problems connected with the current distribution. Both inhomogeneities and external contacts are expected to lead to the same effect; the development and propagation of heat in isolated areas which may spread to destroy superconductivity before the critical density characteristic of most of the material is reached. If the superconducting sample is in the form of a flat strip, or, equivalently, in the form of a thin film ring carrying an induced annular current, instabilities may be expected from the nature of the current distribution alone, for in these cases the current peaks in the edges where the film is most nonuniform.

We have performed some critical current measurements on tin and indium which largely avoid the above experimental complications. The critical current density is induced in a thin film as the image current of a flat ribbon shaped in the form of a closed loop. If the film and the loop are properly dimensioned and the loop is positioned as closely as possible to the film, then one has a situation in which the highest current density occurs well away from the boundaries and once more is reached without the need to attach leads to the specimen. We have also paid particular attention to the sample preparation procedure. Be it said at the outset, however, that we did encounter a serious problem which we believe is connected with the metastability of the superconducting state in our experimental arrangement.

II. EXPERIMENTAL DETAILS

The cryostat used for these experiments is shown in Fig. 1. It consisted of a conventional glass liquid-helium cryostat (bottom section), an evaporator (middle section), and a liquid-nitrogen cryostat (top section). The liquid-nitrogen Dewar could be inserted into the liquid-helium Dewar below through the double O-ring seal above the evaporator. This arrangement allowed making the film in place, permitted subsequent annealing over any temperature interval between 78 and 350 °K in high vacuum and finally made it possible to measure its superconducting properties while in contact with liquid helium. The system could be pressurized slowly with helium gas while keeping the temperature of the film below 80 °K. Magnetic shields reduced the external fields by a factor of 10^{-5}. The shields had a maximum self-field of 80 γ perpendicular to the axis, which was found not to interfere with the critical current measurements.

A 1000-cps alternating current signal of triangular wave form was applied to the gold loop, the "drive coil," shown in Fig. 2. This current was imaged in the superconducting film. The substrate supporting the film formed a window in the copper substrate holder through which the drive coil could "see" a pickup coil which was mounted directly behind the substrate. A microm-

eter-controlled feed mechanism served to move the drive coil into position over the film after the evaporation. As the peak-induced current in the film became critical at a given temperature, some magnetic flux penetrated the film and was detected by the pickup coil. Both the pickup signal, after amplification by a Keithley Model 103 low-noise amplifier, and the input current, as indicated by the voltage drop across a 1-Ω resistor in series with the drive coil, were displayed on a dual beam oscilloscope. The first appearance of a signal on the pickup coil, a small spike (see Fig. 3), was taken as the criterion for the critical current state of the film.

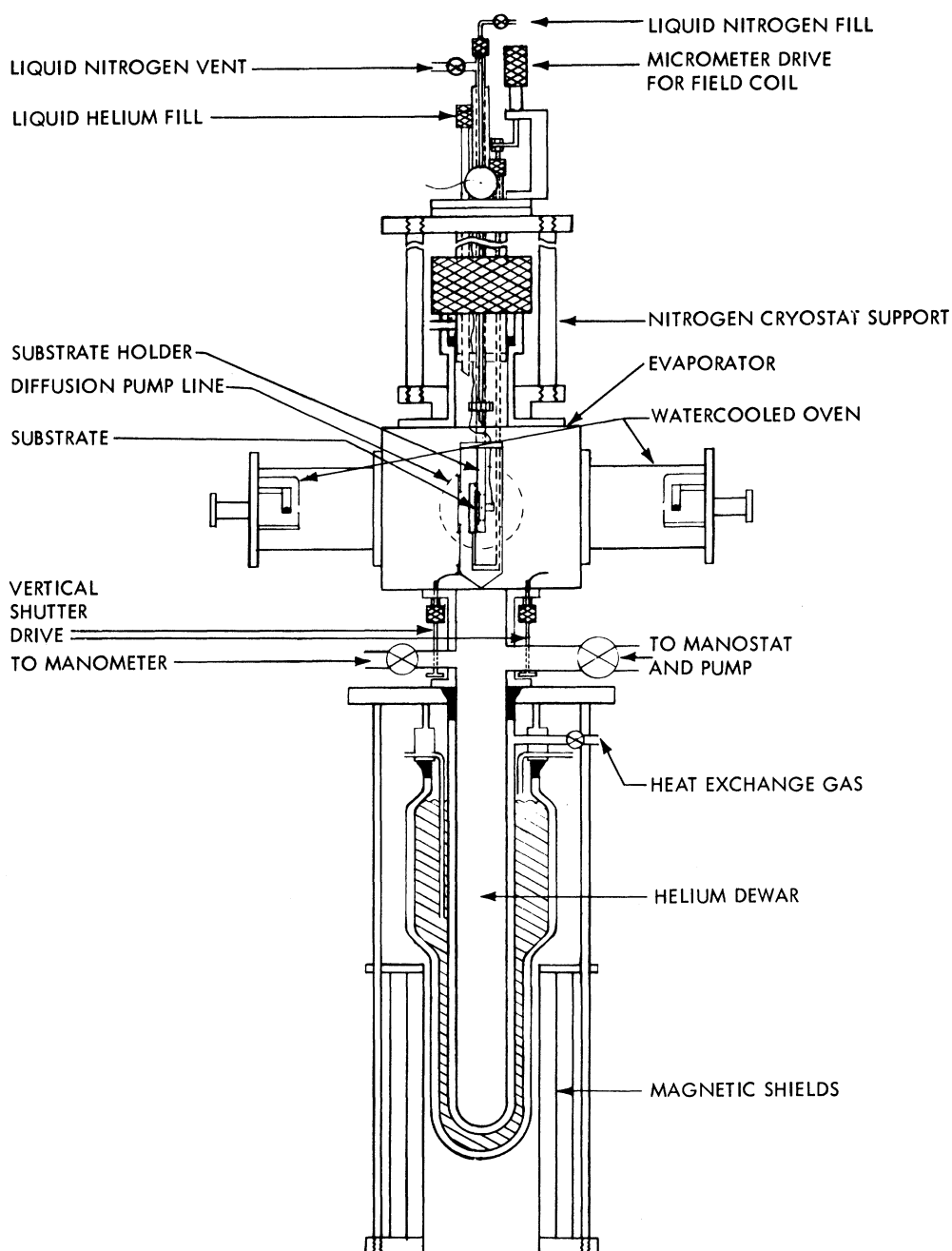The minimum detectable magnetic field through the film at 1000 cps, as determined by the mini-

FIG. 1. Cryostat.

FILM STRIP
(1/16 in. WIDE x 7/8 in. LONG)

DRIVE COIL   1

MAIN FILM
(3/4 in. WIDE x 7/8 in. LONG)

GOLD ELECTRODES

2

3

1 & 4 - CURRENT LEADS
2 & 3 - POTENTIAL LEADS

GLASS

DRIVE COIL
POTENTIAL LEADS

4

SAPPHIRE
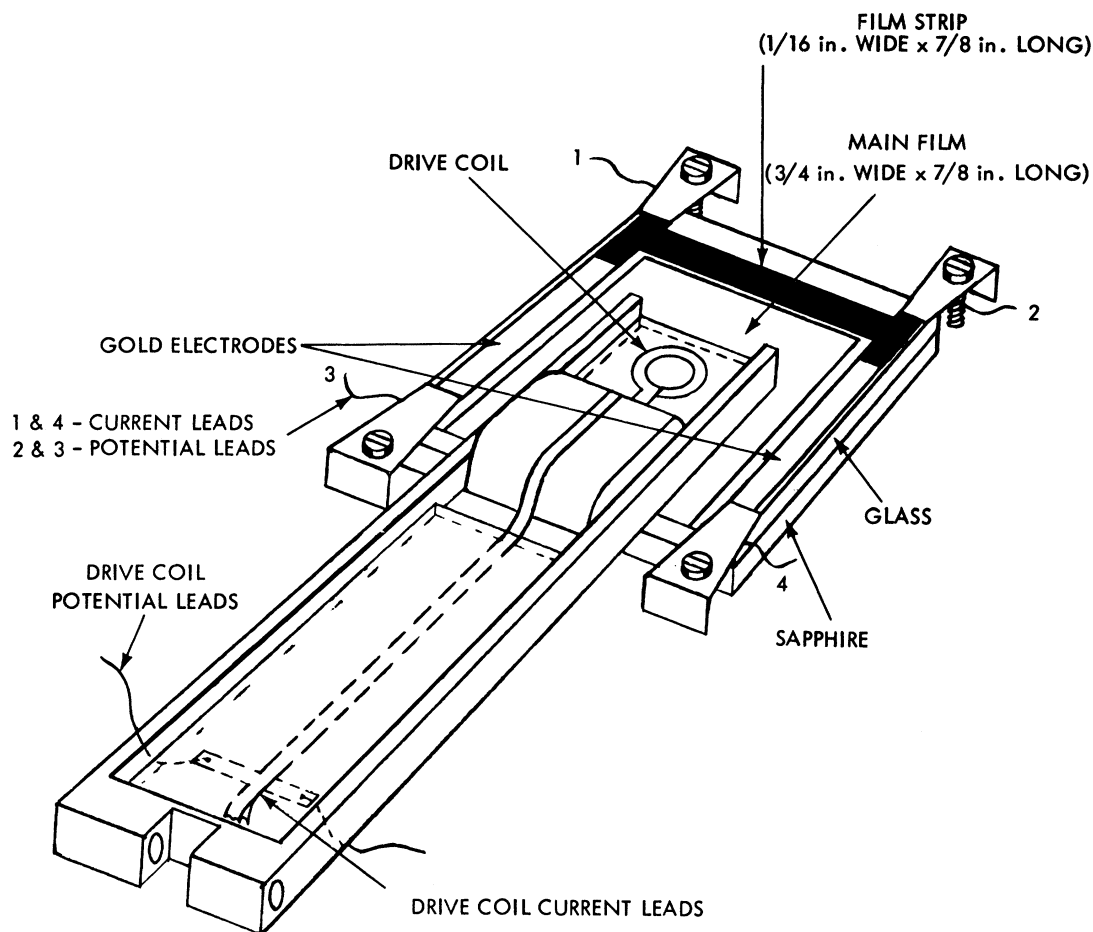
DRIVE COIL CURRENT LEADS

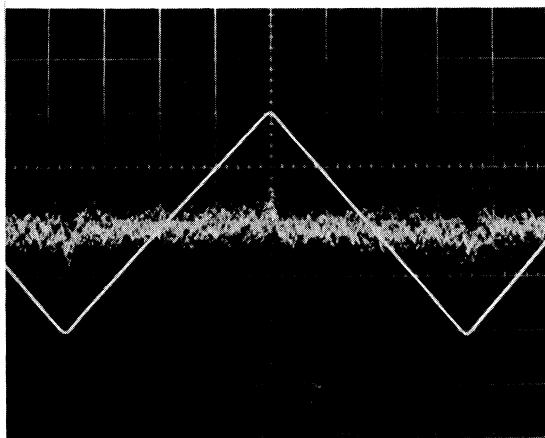FIG. 2. Drive-coil assembly with evaporated films.

FIG. 3. Oscilloscope traces of the pickup signal and the applied current waveform (the triangular wave), at 1 kc/sec, for tin and indium films annealed to temperatures below 200 °K. The applied current amplitude is just supercritical (by <1%). Pickup signal: 10 mV/cm. Applied current: 200 mA/cm. Each large division = 1 cm.

mum detectable pickup voltage, was 2×10^{-3} Oe peak to peak at an input current of 2×10^{-3} A peak to peak. The minimum detectable pickup voltage, conveniently defined here as twice the background noise voltage on the scope (Tektronix 502A) was in turn determined by the following dimensions and relative position of the drive coil and the pickup coil. The drive coil consisted of a 7-mm-mean-diam by 1-mm-wide gold loop. A typical distance between the drive coil and the film was 0.4 mm. The distance between the film and the center of the pickup coil was 6.4 mm. Maximum coupling between the coils was obtained for a pickup coil 4.8 mm long by 2.4 mm i.d. by 8 mm o.d. Several hundred turns of No. 38 copper wire yielded a pickup coil self-inductance of 800 μH.

Between 77.3 and 180°K, the temperature of the film was measured with a copper coil thermometer. In the helium temperature range the temperature was inferred from the vapor pressure of the bath, with an estimated accuracy of 3×10^{-3} °K. It was found convenient to measure the tran-

sition temperature magnetically by slowly lowering the temperature of the film through the transition while looking for the appearance of a small distortion in the normal-state square-wave pickup waveform at the zeros of the applied current. The applied current level for this measurement was set at 50 mA peak to peak, corresponding to the critical current at $T_c - T \simeq 0.01$ °K. It was found impossible to locate the transition within less than $\Delta T = 0.01$ °K by making critical current measurements in this temperature interval near T_c. At $T_c - T \simeq 0.01$ °K the penetration depth increases rapidly and the current distribution spreads into the boundaries of the sample.

The lower end of the temperature interval spanned by these measurements was fixed by the power dissipated in the drive loop. The drive loop was cut out of 0.001-in.-thick, 99.99% pure gold foil, and its resistance was $< 10^{-4}$ Ω at 4.2 °K. A 0.2-mm-thick sheet of Mylar served as thermal insulation between the loop and the film. The measurements were terminated at a peak input current of order 1 A. Depending on the film thickness, the residual resistivity of the film, and the separation between drive coil and film, this limit implied that a temperature interval of 1–2 °K was covered. From the input current amplitudes and the milliampere pickup sensitivity cited above, one infers that, except perhaps for the first point near T_c, the accuracy with which the critical drive coil current could be measured was determined by the accuracy with which the corresponding voltage on the scope could be read, ±1%.

The substrate consisted of a sandwich of 1.5 mm of sapphire and 1 mm of microscope glass bonded together with a thin layer of RTV cement (RTV-112, General Electric Co.). The sapphire provided an essentially isothermal surface behind the glass during the evaporation of the films. The finished sandwich could be cleaned easily with detergent in an ultrasonic cleaner after precleaning with chromic acid. Final cleaning was done with a vapor degreaser operating with isopropyl alcohol. The substrates were mounted in a dust-free enclosure and the surfaces were treated with a film of collodion just before closing the shutters of the heat shield.

Tin (99.9999% Vulcan Detinning Co.) or indium (99.9999% Comico Co.) was evaporated from tungsten filaments onto the glass surface of the substrates held at 80 °K in a vacuum of 10^{-7} mm Hg and at an average rate of 50 Å/sec. During several experiments a film of SiO was evaporated first. After the evaporation of the metal, the films were annealed to some temperature below 180 °K in a vacuum of 10^{-7} mm Hg. In some cases they were immediately cooled to helium tempera-

tures. After the first critical current run the film was allowed to warm up to a temperature near 180 °K in a vacuum of 5×10^{-6} mm Hg. Subsequently, the critical current of the annealed film was measured. An annealing record corresponding to one of the films in Table I ($T_{c1} = 4.171$ °K, $T_{c2} = 3.865$ °K) is shown in Fig. 4. Resistance measurements were made on a simultaneously deposited auxiliary film strip shown in Fig. 2. The large length-to-width ratio of the auxiliary strip was required for reliable resistivity estimates (Table I).

Film thicknesses and uniformity were measured interferometrically. In order to obtain uniformly thick films the distance between the substrate and the evaporator was generally 20 cm. Left-right uniformity was improved by using two filaments side by side, and vertical uniformity was improved by closing the shutter across the beam from top to bottom. The films were found to be uniform within 10%.

III. EXPERIMENTAL RESULTS AND DISCUSSION

The temperature dependence of the critical current density was obtained by fitting the expression $J_c(T) = J_{c00}(1 - t^2)^\alpha (1 + t^2)^{1/2}$, $t \equiv T/T_c$, to the experimental data. Critical current densities were derived from the experimentally measured critical drive-coil currents $I_c(t)$ with the aid of a theoretical relation of the form $J_c(t) = a(t)I_c(t)$ (cf. Appendix), where the coefficient $a(t)$ describes the spread of the current distribution in the film.

With $\alpha = \frac{3}{2}$, $J_c(t)$ has the Ginzburg-Landau temperature dependence. Other temperature dependences were tried: $(1 - t^2)^{3/2}$, $(1 - t)^{3/2}$. Neither one of these nor $(1 - t^2)^{3/2}(1 + t^2)^{1/2}$ gave a good fit to the data over the whole temperature interval. It was decided therefore to determine the exponent α and the coefficient J_{c00} by means of a two-parameter least-squares fit. Upon varying the transition temperature slightly in steps of 0.001 °K in the neighborhood of its measured value, it was found that the mean-square error would go through a minimum. The value of T_c at the minimum was usually within -0.005 °K of the measured transition temperature and this value was used in the final expression for $J_c(t)$. The quantities α, T_c, and $J_{c0} \equiv 2^{\alpha+1/2} J_{c00}$ are entered in Table I. Plots of the corresponding expressions for the critical current densities of two of the films in the table, tin, $T_c = 4.215$ °K, and indium, $T_c = 3.824$ °K, together with the data points, are shown in Figs. 5 and 6. The quality of the fit varied only slightly from film to film with a minimum in the mean-square deviation at the annealed indium film, $T_c = 3.559$ °K, and a maximum at the unannealed indium film, $T_c = 3.778$ °K. With the exception of

TABLE I. Compendium of data on tin and indium films deposited at 80 °K and annealed to temperatures below 200 °K. The symbols are defined in the text.

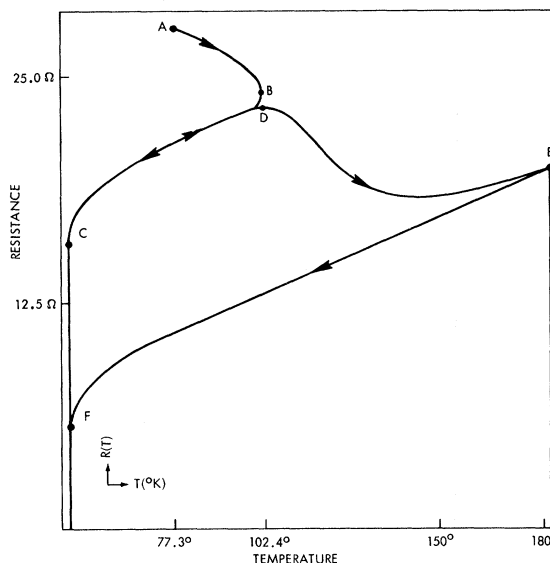| J_{c0}^{theor} (10^7 A/cm²)	J_{c0}^{expt} (10^6 A/cm²)	$J_{c0}^{expt}/J_{c0}^{theor}$	J_{c0}^{expt} (10^6 A/cm²)	α	T_c (°K)	T_A (°K)	d (Å)	ρ_0 (10^{-6} Ω cm)	λ_{eff}^0 (Å)	l_{eff} (Å)	Substrate
Tin											
1.21	6.19	0.51	1.87	1.22	4.215	110	480	8.27	2950	130	1000 Å of SiO on glass
1.91	7.54	0.39	2.28	1.23	3.898	180	480	3.06	1870	340	1000 Å of SiO on glass
1.28	6.16	0.48	1.86	1.23	4.171	100	550	7.34	2790	140	1000 Å of SiO on glass
2.03	8.05	0.40	2.48	1.20	3.865	180	550	2.69	1770	390	1000 Å of SiO on glass
1.48	5.85	0.40	1.78	1.23	4.259	80	930	5.53	2440	190	Glass
1.11	6.92	0.62	2.01	1.28	4.243	95	1050	9.88	3210	110	Glass
1.65	5.10	0.31	1.68	1.10	3.931	120	930	4.14	2140	250	5000 Å of SiO on sapphire
Indium											
1.34	8.80	0.66	2.79	1.16	3.824	80	400	4.83	2800	210	1500 Å of SiO on glass
1.84	10.60	0.58	3.34	1.16	3.559	180	400	2.40	2050	430	1500 Å of SiO on glass
1.46	9.65	0.66	3.07	1.15	3.778	80	620	4.05	2580	250	Glass
2.25	10.80	0.48	3.63	1.08	3.493	175	620	1.57	1720	660	Glass

FIG. 4. Resistance of a tin film as a function of temperature. The film was deposited at temperature A, was annealed to B and cooled to C, $T_c = 4.171$ °K. After the first critical current run below T_c the film was warmed up to D along CD and was annealed to E. It was then cooled to F, $T_F = 3.865$ °K for the second critical current run below T_F. See Table I, entries 3 and 4, for additional data on this film.

the last tin film in the table (see below) the exponents for tin are within 5% of the mean value 1.23. Again with the exception of the last indium film (see below), the exponent for indium is 1.16.

When $J_c(t)$ is extrapolated to the neighborhood of T_c, it becomes possible to compare the new constant $J_{c0} = J_{c00}2^{\alpha + 1/2}$ in $J_c(t) \approx J_{c\,0}(1-t)^\alpha$ with the corresponding constant in the theoretical expression $J_c(t) = J_{c0}(1-t)^{3/2}$ given by Maki[13] (only approximately so, since the measured exponent $\neq \frac{3}{2}$). Maki's value for $J_{c0}^{theor} = 0.37 \times H_c(0)\,(\Delta_0/\rho_0 \hbar)^{1/2}$ is entered in Table I. [$H_c(0)$ is the thermodynamic critical field at $T = 0$, ρ_0 is the residual resistivity, $\Delta_0 = 1.75\,k_B T_c$, k_B is the Boltzmann constant. The form of J_{c0}^{theor} follows from the one given in Eq. (23) of Ref. 13;

$$J_c(t) = \frac{ne}{m}\,\frac{\pi k_B T_c}{V_F}\left(\frac{\tau \pi k_B T_c}{\hbar}\right)^{1/2}(1-t)^{3/2},$$

by making the simple substitutions $\Delta_0 = 1.75\,k_B T_c$, $V_F \tau = l_{eff}$ and $mV_F/ne^2 = l_{eff}\,\rho_0 \cong 10^{-11}$ Ω cm².] The measurements are seen to be low by a factor ≈ 2. Values of J_{c0} in $J_c(t)$ near T_c derived from the Ginzburg-Landau[11] form

$$J_c^{GL}(t) \approx (1-t^2)^{3/2}(1+t^2)^{1/2}$$
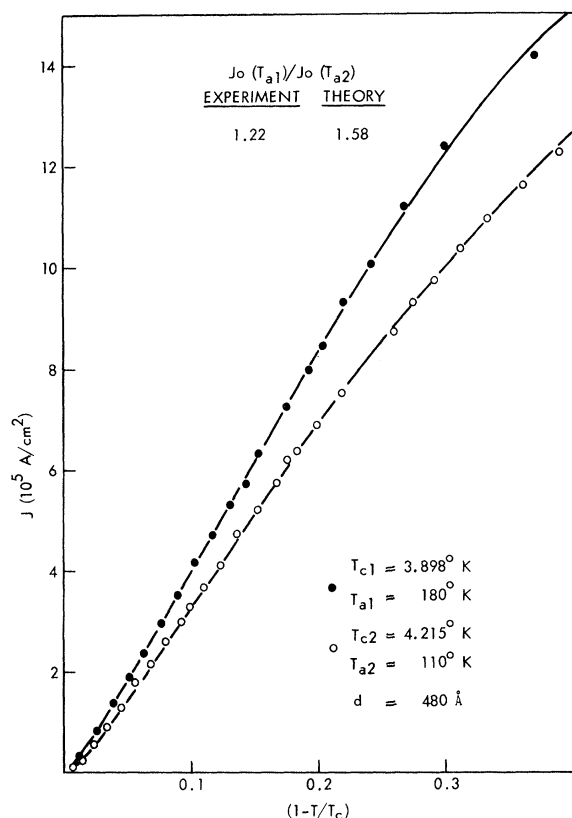
and from the Bardeen[11] form

FIG. 5. Critical current density of a tin film condensed at 80 °K and annealed to temperature T_a. Data on this film are collected in Table I, entries 1 and 2.
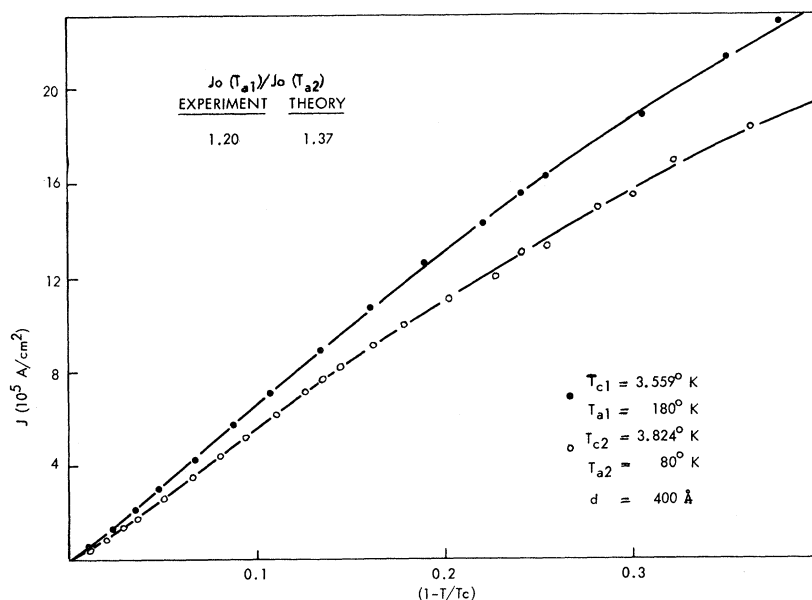
$$J_c^B(t) \approx (1 - t^2)^{3/2}$$

are larger than J_{c0}^{theor} given by Maki; $J_{c0}^{theor} = 0.26\ J_{c0}$ (Bardeen) $= 0.34\ J_{c0}$ (Ginzburg-Landau). Hence the discrepancies between these latter estimates and our results are correspondingly larger.

Inserts in the figures give experimental and theoretical ratios of the critical current amplitudes before and after annealing. Theoretically the amplitudes should scale as

$$[(T_c l_{eff})_1 / (T_c l_{eff})_2]^{1/2},$$

where l_{eff} is the electronic mean free path, which was estimated by using the measured residual resistivity in $\rho_b l_b = \rho_0 l_{eff}$ where $\rho_b l_b = 1.05 \times 10^{-11}$ $\Omega\ cm^2$ and $(1.03 \pm 0.23) \times 10^{-11}\ \Omega\ cm^2$ for tin[14] and indium,[8] respectively. As the inserts show, the experimental ratio of the critical current amplitudes before and after annealing was low compared to the predicted value. That this was true in general for these films may be seen from the ratio $J_{c0}^{expt}/J_{c0}^{theor}$ in Table I. $J_{c0}^{expt}/J_{c0}^{theor}$ decreases with annealing to higher temperatures. (Tin films Nos. 5–7 were all separate films and hence cannot be compared.) This result might be interpreted to suggest that the critical current amplitude depends less strongly on the electronic mean free path than is implied by the above theoretical ratio. However, the percent deviation of J_{c0}^{expt} from the theoretically predicted value varied, and hence an equally plausible explanation of this observation would be that some structural changes occurred in the films during annealing which did affect the critical current but did not show up strongly in the residual

FIG. 6. Critical current density of an indium film condensed at 80 °K and annealed to temperature T_a. Data on this film are collected in Table I, entries 8 and 9.

resistivity. Even though these films had been annealed to temperatures below the critical temperature for agglomeration, 200 °K, some structural inhomogeneities may have developed between runs. In the case of tin, discontinuities in the substrate surface due to surface flaws or dust have been observed[15] to develop voids in the film upon annealing to temperatures below 150 °K. This is assumed to be equally true for indium. In particular, it may explain the low values of J_{c0} and α observed for the last indium film in the table.

The last entry for tin in the table illustrates the effect of a particular kind of substrate surface defect on the critical current density. Both J_{c0} and α are below average for this film. In general, when polished substrates such as quartz or sapphire were used, the critical currents were always much lower than those indicated in Table I. Tin in particular "decorated" the polishing scratches like any other discontinuity, probably to some extent already during deposition. For this reason surfaces containing line discontinuities like the polishing scratches on the best available sapphire or crystal quartz plates (polished to 1μ in. optical flatness) could not be used for these experiments. Not even a film of 5000 Å of SiO was effective in smoothing the polishing scratches on such a sapphire plate, as demonstrated by the results for the last tin film in Table I.

The measurements were complicated by flux trapping. However, trapped flux showed up as an asymmetry in the pickup waveform and was therefore easily detected. It could be removed by either heating the film above its transition temperature after every measurement or by momentarily moving the drive coil to a different position over the film. The resulting slightly changed interaction of the trapped flux with the field of the drive coil was often sufficient to dislodge this flux and effectively eject it from the film.

The critical current amplitude depended strongly on the relative position of the drive coil and the film for most of the films. Even if the coil was moved in the vicinity of the center of the film, the critical current amplitude fluctuated. The amplitude variations were studied carefully in several experiments. We concluded that they were simply due to sample defects in the current path. The current distribution in the films is unstable in this experimental situation and hence is expected to be especially sensitive to sample defects. The current density given in this work is therefore the maximum critical current density attained in each sample. The possibility that there was some residual interference with the critical current state from microscopic and submicroscopic structural inhomogeneities even at the position of maximum critical current cannot be ruled out.

IV. INTERPRETATION AND CONCLUSIONS

We put our work into perspective by briefly comparing it with related critical current measurements. In experimental situations in which the change in magnetic field energy at the superconducting transition is comparable to the condensation energy plus the kinetic energy of the superconducting current, essentially two difficulties arise. If the film is evaporated in the form of a cylinder and if an external current is directly injected, then there are not only electrical contact problems, but because of thermal contact problems during evaporation an inhomogeneous and coarse-grained film structure may result.[2] If the film is simply a long strip which might be of order millimeters wide, then the maximum current density occurs in the edges where the film is most nonuniform. Nevertheless, large critical current densities which are in complete agreement with Bardeen's expression for

$$J_c^B(t) = \tfrac{1}{2} H_c(0) (\sigma \Delta_0/\hbar)^{1/2} (1 - t^2)^{3/2}$$

have been measured with the latter arrangement.[6] Looking back at the discussion in Sec. III shows that these critical current densities are roughly eight times larger than the ones obtained in the present experiment. It might be pointed out, however, that the conversion from currents to current densities in Ref. 6 involved a large and only approximately known geometrical factor. The possibility that fluxoids had entered the film before the critical current state was reached can also not be excluded.

If the experimental arrangements are such that the change of magnetic field energy at the transition dominates the total energy change, an additional complication arises from the metastability of the superconducting state. Experiments using a thin film cylinder in an axial magnetic field, as well as our own experiment, suffer from this difficulty. Since the superconducting cylinder is the thin film strip doubled back on itself, experiments on cylindrical films in axial fields also suffer from the edge problem. A rough estimate of the densities to be expected in such an experiment, using the data given in Ref. 5, shows that the measured densities are low by a factor of 7 compared to $J_c^B(t)$. Hence they are of the same order of magnitude as those measured here. In spite of these rather low values it has been argued elsewhere[16] that the metastable limit, or the depairing maximum in the current density, [13] was indeed reached in that experiment. With respect to our own experiment we hesitate to make this assertion. Rather, we suggest that the critical current tran-

sition may have been masked to some extent by the metastability of the superconducting state of the film in the field of the drive coil. The depairing maximum of the current density may not quite have been reached. Our interpretation of the amplitude variations of the critical current with relative position of drive coil and film agrees with this point of view. The observation of different temperature dependences of the critical current in tin and indium and the fact that the exponent in $(1-t)^{\alpha}$ was observed to be smaller than the theoretically predicted value of 1.5 for both metals further supports this conclusion.

All of these experimental problems can be eliminated in principle with the use of a superconducting thin film bridge which is only of order microns wide.[9] In addition, current density gradients (present in our work) and gradients in the order parameter transverse to the flow momentum, which would increase the energy in the superconducting state through $|\nabla\psi|^2$, are largely eliminated with the "bridge method." If such a bridge is narrow enough the critical depairing maximum can be reached before the self-field of the current becomes large enough to form fluxoids which just fit inside the bridge. Current densities measured with this method fit the Ginzburg-Landau expression for

$$J_c^{GL}(t) = (\tfrac{2}{3})^{3/2} \tfrac{1}{2} H_c(0)$$

$$\times \left(\frac{\sigma\Delta_0}{\hbar}\right)^{1/2}(1-t^2)^{3/2}(1+t^2)^{1/2}$$

rather well. They are therefore roughly by a factor of 6 higher than those measured in this work. It also follows that if this latter work is taken to be the most definitive statement on these experiments, then Maki's estimate of the critical current density near T_c may be somewhat low.

ACKNOWLEDGMENTS

APPENDIX

The coefficient $a(t)$ in the relation between $J_c(t)$ and $I_c(t)$ given in the text was derived in first approximation to the electromagnetic boundary value problem corresponding to this experimental arrangement. We write the Ginzburg-Landau equation for the vector potential inside the film in first approximation:

$$\nabla\times\nabla\times A = [\psi_0^2/\lambda^2(t)]A .$$

ψ_0^2 is constant throughout the film and is strictly equal to unity in this approximation. However, according to the nonlinear theory for current flow in an infinite thin film superconducter, ψ_0^2 should be $=\tfrac{2}{3}$ at the critical point.[11] A better estimate of λ at the critical point would therefore be $\lambda_{eff}=\lambda\sqrt{\tfrac{3}{2}}$. We make this correction in calculating $J_c(t)$. Note also that ψ_0 is real here, corresponding to a situation with no flux quanta inside the film.

Solving the problem in cylindrical coordinates with the center of coordinates at the center of the film and the z axis normal to the film and concentric with the axis of the drive loop at $z=+z_0$, $a_2 \geq r \geq a_1$, yields

$$J = J(z,r,t)\hat{\theta} = -(I\beta^2/W)\int_{a_1}^{a_2}\int_0^\infty J_1(aq)$$

$$\times J_1(rq)e^{-q\Delta} Q(z,d,\beta,q)\,dq\,a\,da ,$$

where I is the input current, W is the drive-coil width, d is the film thickness,

$$Q(z,d,\beta,q) = \{\beta^2(q)\sinh[(q^2+\beta^2)^{1/2}(z+\tfrac{1}{2}d)]$$

$$+\beta(q)\cosh[(q^2+\beta^2)^{1/2}(z+\tfrac{1}{2}d)]\} /$$

$$\{[(\beta^2(q)+1)]\sinh[d(q^2+\beta^2)^{1/2}]$$

$$+2\beta(q)\cosh[d(q^2+\beta^2)^{1/2}]\} ,$$

$$\beta^2(q) = q^2/(q^2+\beta^2) , \quad \Delta=(z_0-\tfrac{1}{2}d) ,$$

$$\beta = 1/\lambda_{eff}(t) .$$

Now consider the case $q/\beta \ll 1$ and $10^{-5}\leq\lambda\leq10^{-2}$ cm, which is not a significant restriction. The response current density of the film is then given by

$$J = -\frac{I\beta}{W}\int_{a_1}^{a_2}a\,da\int_0^\infty J_1(qa)J_1(qr)e^{-q\Delta}$$

$$\times\frac{q[\cosh(z+\tfrac{1}{2}d)\beta]/\sinh d\beta}{1+(2q/\beta)\coth(d\beta)}\,dq ,$$

neglecting terms of order $(q/\beta)^2$. In order to facilitate the integration we replace the fraction $1/[1+(2q/\beta)\coth d\beta]$ by

$$\exp[-(2\ln2)(q/\beta)\coth d\beta] .$$

These two expressions are equal at

$$q=\{0, \beta/2\coth d\beta\} .$$

Note that for

$$q\geq\beta/2\coth d\beta$$

or for $q/\beta\approx1$ the exponential $e^{-q\Delta}$, and in any case the Bessel functions, will reduce the integrand to zero. Hence writing

$$J = -\frac{I\beta\cosh[(z+\tfrac{1}{2}d)\beta]}{W\sinh d\beta}$$

$$\times \iint a\,da\,q\,dq\,J_1(qa)J_1(qr)e^{-qY} \quad ,$$

where $Y = \Delta + [(2\ln 2)/\beta]\coth d\beta$,

one obtains

$$J = -P\int_{a_1}^{a_2} a\,da\,\frac{Y}{\pi(ar)^{3/2}}\,\frac{Q^1_{1/2}(\gamma)}{(\gamma^2-1)^{1/2}} \quad ,$$

where $\gamma^2 = \dfrac{a^2 + r^2 + Y^2}{2ar}$

and $P = -\dfrac{I\beta\cosh[(z+\frac{1}{2}d)\beta]}{W\sinh d\beta}$

and $Q^1_{1/2}(\gamma)$ is the Legendre function of the second kind. This function may be expressed in terms of complete elliptic integrals, K and E:

$$J = -P\int_{a_1}^{a_2} a\,da\,[Y/\pi(ar)^{3/2}]$$

$$\times(k/4k'^2)[2k'^2K - (1+k'^2)E] \quad ,$$

where $k^2 = [4ar/Y^2 + (a+r)^2]$

and $k'^2 = 1 - k^2$.

It is of interest to consider the limiting value of this integral as $a, r \gg Y$ and $a \approx r$. In that case $k^2 \approx 1$ and $k'^2 \approx 0$. Expanding K and E near $k'^2 \approx 0$, one has

$$J = -P\int_{a_1}^{a_2} a\,da\,(Y/2\pi)\,[k/(ar)^{3/2}]$$

$$\times[-1/2k'^2 + \tfrac{3}{4}(x-\tfrac{1}{2}) + O(xk'^2)] \quad ,$$

where $x = \ln(4/k')$, and substituting the values for the parameters k and k' one obtains

$$J = -P\int_{a_1}^{a_2} \frac{Y\,da}{\pi r(a+r)}\,\left(-\tfrac{1}{2}\,\frac{(a+r)^2}{[Y^2+(a-r)^2]} + \tfrac{3}{4}\{[(\ln 4\right.$$

$$\left. -\tfrac{1}{2}) - \tfrac{1}{2}\ln[Y^2 + (a-r)^2] + \ln(a+r)]\}\right) \quad .$$

Here $Y^2 + (a+r)^2 \approx (a+r)^2$ has been used. Since the terms containing $(a+r)$ vary little, we set $(a+r) = 2r$. Introducing new variables

$$s \equiv Y/\tfrac{1}{2}W, \quad x = (a-r)/\tfrac{1}{2}W, \quad z = r/\tfrac{1}{2}W \quad ,$$

we integrate to obtain

$$J = -P\left[\frac{3s}{4\pi z^2}(\ln 4 - \tfrac{3}{2})\right.$$

$$+\frac{1}{\pi}\left(1+\frac{3s^2}{8z^2}\right)\tan^{-1}\frac{2s}{x_2 x_1 + s^2}$$

$$\left.+\frac{3s}{16\pi z^2}\left(x_2\ln\frac{x_2^2+s^2}{(2z)^2} - x_1\ln\frac{x_1^2+s^2}{(2z)^2}\right)\right] \quad ,$$

where $x_{1,2} = (a_{1,2}-r)/\tfrac{1}{2}W$. Keeping in mind that $s \approx 1$ and $z \approx 10$, we see that the current density is equal to

$$J \simeq \frac{I\beta}{W}\,\frac{\cosh[(z+\frac{1}{2}d)\beta]}{\sinh d\beta}$$

$$\times\frac{1}{\pi}\tan^{-1}\frac{WY}{(a_2-r)(a_1-r)+Y^2} \quad .$$

The neglected terms give corrections of order 10% to J owing to the finite drive-coil radius. The term kept is the solution for the infinite strip line over a superconducting thin film ground plane; it is the only term which does not go to zero in the limit $a \approx r \to \infty$. Finally, the last expression for J may be written

$$J(x, z, t) \simeq \frac{I}{\lambda_{eff}(t)W}\,\frac{\cosh[(z+\frac{1}{2}d)/\lambda_{eff}(t)]}{\sinh[d/\lambda_{eff}(t)]}$$

$$\times\frac{1}{\pi}\tan^{-1}\left(\frac{WY(t)}{x^2+Y^2(t)-(\frac{1}{2}W)^2}\right) \quad ,$$

where $x \equiv \frac{1}{2}(a_1+a_2)-r$. $J(x, z, t)$ has a maximum at $(z, x) = (\frac{1}{2}d, 0)$ and we define $a(t)$ by

$$J_{max}(t) \equiv a(t)I,$$

$$a(t) = \frac{\coth[d/\lambda_{eff}(t)]}{W\lambda_{eff}(t)}\,\frac{1}{\pi}\tan^{-1}\left(\frac{WY(t)}{Y^2(t)-(\frac{1}{2}W)^2}\right) \quad .$$

$a(t)$ turned out to be $\approx 0.6/Wd$ throughout the whole temperature interval covered by the measurements. Now $J_{max}(t) = J_c(t)$ for $I = I_c(t)$, i.e.,

$$J_c(t) = a(t)I_c(t) \quad . \tag{A1}$$

The calculation has been given in some detail in order to exhibit the approximations made to obtain Eq. (A1). Without going into detailed error estimates we merely note that the approximations depend on $\lambda < \Delta \simeq \frac{1}{2}W/\ll a, r$, and that these conditions are indeed fairly well satisfied in this experiment. The real limit of accuracy of the experiment may lie in the measurements, by virtue of the metastability of the superconducting state – not in formula (A1).

In conclusion it should perhaps be pointed out as a matter of some independent interest that one is dealing in these experiments with a situation of strong magnetic field attenuation. Even though our films are much thinner than the penetration depth λ_{eff}, the magnetic field anywhere behind the film is smaller by at least a factor of 10^{-3}–10^{-4} compared to the strongest fields in front of the film. The fields inside the film may readily be derived from the expressions for $J(x, z, t)$ given above. A general discussion of the magnetic shielding strength of thin-walled superconducting shells has been given elsewhere.[17]

*Submitted to the University of Maryland in partial fulfillment of the requirements for the Ph. D. degree in physics.

[1]N. E. Alekseevski and M. N. Mikheeva, Zh. Eksperim. i Teor. Fiz. 31, 951 (1956) [Soviet Phys. JETP 4, 810 (1957)].

[2]N. I. Ginzburg and A. I. Shalnikov, Zh. Eksperim. i Teor. Fiz. 37, 399 (1959) [Soviet Phys. JETP 10, 285 (1959)].

[3]N. E. Alekseevski and M. N. Mikheeva, Zh. Eksperim. i Teor. Fiz. 38, 292 (1960) [Soviet Phys. JETP 11, 211 (1960)].

[4]J. E. Mercereau and L. T. Crane, Phys. Rev. Letters 9, 381 (1962).

[5]J. E. Mercereau and T. K. Hunt, Phys. Rev. Letters 8, 243 (1962).

[6]R. E. Glover III and H. T. Coffey, Rev. Mod. Phys. 36, 299 (1964).

[7]W. H. Meiklejohn, Rev. Mod. Phys. 36, 302 (1964).

[8]R. D. Chaudhari and J. B. Brown, Phys. Rev. 139, A1482 (1965).

[9]T. K. Hunt, Phys. Rev. 151, 325 (1966).

[10]V. L. Ginzburg and L. D. Landau, Zh. Eksperim. i Teor. Fiz. 20, 1064 (1950).

[11]J. Bardeen, Rev. Mod. Phys. 34, 677 (1962).

[12]K. T. Rogers, Ph. D. thesis, University of Illinois, 1960 (unpublished).

[13]K. Maki, Progr. Theoret. Phys. (Kyoto) 39, 333 (1963).

[14]D. K. C. McDonald, Handbuch der Physik (Springer, Berlin 1956), Vol. 14, p. 137.

[15]P. Scharnhorst, Surface Sci. 15, 380 (1969).

[16]D. H. Douglass, Jr., Phys. Rev. 132, 513 (1963).

[17]P. Scharnhorst, Naval Ordnance Laboratory Technical Report No. 70-4, 1970 (unpublished).

Ultrasonic Attenuation in Dirty Superconductors

R. Guermeur,* J. Joffrin, and A. Levelut

Laboratoire d'Ultrasons,[†] Faculté des Sciences de Paris, Tour 13, 9 quai Saint-Bernard, Paris 5e, France

(Received 8 January 1970)

Experimental support for the theory of the attenuation α of ultrasonic waves in dirty superconductors has been obtained with 10-GHz longitudinal waves in mercury-indium alloys. α varies as $H_{c2} - H$ near H_{c2} and the slope $\Delta\alpha/\Delta H$ has the predicted value.

The ultrasonic attenuation in clean second-type superconductors versus biasing magnetic field H has been studied theoretically[1] and experimentally[2] in the vicinity of H_{c2}. It varies as $(H_{c2} - H)^{1/2}$. In a dirty superconductor, the theory[3,4] predicts a linear variation versus $\Delta H = H_{c2} - H$.

The aim of this paper is to report on experimental results which confirm this theory.

This theory has been developed within the following hypothesis: The mean free path l of the electrons is small compared to the coherence length ξ_0; the electronic Green's functions are supposed independent of H because $\omega_c l \ll v_F$, and the gap $\Delta(r)$ on which they are dependent is slowly varying on distances of the order of $(l\xi_0)^{1/2}$; the correlation functions of the electronic density are completely screened when the ultrasonic frequency ω is lower than the plasma frequency. These conditions are satisfied in our experiments.

If the two subsidiary conditions $\Delta(r) \ll \pi k T_c$ and $\hbar\omega \ll \pi k T_c$ are fulfilled, in the neighborhood of H_{c2}, the attenuation α_S for longitudinal waves

in the supraconducting phase is given by

$$\frac{\alpha_S(H)}{\alpha_N} = 1 - \frac{1}{4\pi} \frac{e}{\sigma\alpha} \frac{[1 + L(\rho)]}{\beta[2K_2^2(T) - 1]\mu_0} (H_{c2} - H) . \quad (1)$$

In this formula, $\sigma = Ne^2\tau/m^*$ is the electrical conductivity; $\alpha = \frac{1}{3} v_F^2 \tau e H_{c2}(T) \mu_0$; ρ is defined by $\rho = \alpha/2\pi k T$; $L(\rho)$ is a function tabulated in Ref. 3; $\beta = 1.16$; and $K_2(T)$ is the second parameter of Landau-Ginzburg defined by Maki (Ref. 5); the ratio $K_2(T)/K$ has been calculated by Caroli et al. (Ref. 6) where

$$K^2 = \left(\frac{3Ne}{2\pi^2\sigma\hbar}\right)^2 \frac{2\pi m^*}{\mu_0 k_F^5} 7\xi(3) = \frac{14\xi(3)}{\mu_0\pi^4} C(\tau)$$

with $C(\tau) = \dfrac{3m^{*3}}{4e^2\hbar^2(9\pi^7)^{1/3}N^{5/3}\tau^2}$.

Formula (1) may be written in the more compact form

$$\frac{\alpha_N - \alpha_S}{\alpha_N} = \frac{\Delta\alpha(H)}{\alpha_N} = A(T) \frac{\Delta H}{H_{c2}(T)} \quad (2)$$

with

$$A(T) = \frac{3}{4\pi\beta\mu_0} \frac{Ne}{\sigma^2 v_F^2 m^*} \frac{1 + L(\rho)}{2K_2^2(T) - 1} = \frac{C(\tau)}{\beta\mu_0} \frac{1 + L(\rho)}{2K_2^2(T) - 1} .$$
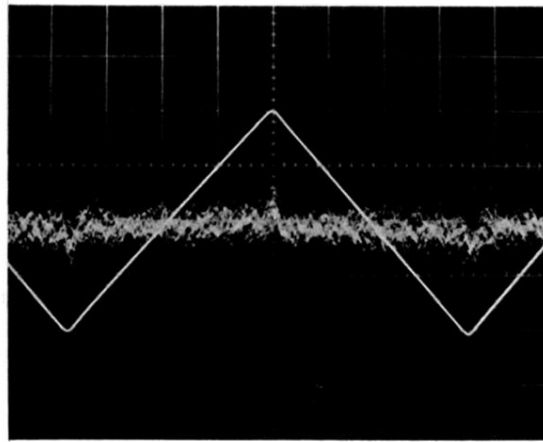
FIG. 3. Oscilloscope traces of the pickup signal and the applied current waveform (the triangular wave), at 1 kc/sec, for tin and indium films annealed to temperatures below 200 °K. The applied current amplitude is just supercritical (by < 1%). Pickup signal: 10 mV/cm. Applied current: 200 mA/cm. Each large division = 1 cm.